Available online at www.CivileJournal.org

Civil Engineering Journal

(E-ISSN: 2476-3055; ISSN: 2676-6957)

Vol. 8, No. 05, May, 2022

# Assessing the Effect of GGBFS Content on Mechanical and Durability Properties of High-Strength Mortars

Si-Huy Ngo [1], Ngoc-Tan Nguyen [2*], Xuan-Hien Nguyen [3]

[1] *Department of Engineering and Technology, Hong Duc University, No. 565, Quang Trung Street, Dong Ve Ward, Thanh Hoa City 40000, Vietnam.*

[2] *Faculty of Building and Industrial Construction, Hanoi University of Civil Engineering, No. 55, Giai Phong Street, Hai Ba Trung District, Hanoi City 10000, Vietnam.*

[3] *Department of Science, Technology and Environment, Ministry of Construction, No. 37, Le Dai Hanh Street, Hanoi City 10000, Vietnam.*

Received 06 February 2022; Revised 22 April 2022; Accepted 28 April 2022; Published 01 May 2022

**Abstract**

As a large amount of steel is produced for the industrialization and modernization of Vietnam, a correspondingly large quantity of steel slag is also released annually. Besides, the demand for mortar is increasing due to urbanization, especially for the high-strength and durability mortar used for important constructions and structures in aggressive environmental areas. This study aims to carry out further research into high-strength mortars incorporating ground granulated blast furnace slag (GGBFS). The control mixture was designed with a water-to-binder ratio of 0.2, and the amount of silica fume used was equal to 25% of the total binder amount by mass. Four other mixtures were designed using GGBFS to substitute for 15, 30, 45, and 60% of cement by mass. The engineering properties of fresh and hardened mortars were comprehensively investigated, especially the durability properties. The microstructure of these mortars was also examined using scanning electron microscopy. Test results show that replacing 15 or 30% of cement with GGBFS yields an improvement in mortar's strength and durability properties. All the mortars in this study show excellent qualities with high strength, low water absorption, and high resistance to chloride attack. Moreover, the presence of GGBFS reduces the shrinkage of mortar caused by the drying process.

*Keywords:* High-Strength Mortar, GGBFS, Drying Shrinkage, Rapid Ion Penetration, Durability.

## 1. Introduction

In recent years, as the economy of Vietnam develops at an increasingly fast pace, the urbanization process is also being focused on more. Consequently, the demand for construction materials is also increasing day by day. Among those, steel and mortar are two of the most popular construction materials. While steel is used as longitudinal and transverse reinforcements to enhance the strength and ductility of the structure, mortar is used as a cover layer to protect the surface of the structure. According to the Vietnam Steel Association, approximately 23.3 million tons of iron and steel were produced, and around 5 million tons of iron and steel slags were also generated in 2018. It is projected that the total amount of these slags will reach 10 million tons in 2025. On the other hand, the demand for cement in the construction industry is also increasing. In 2020, about 100 million tons of cement had been produced in Vietnam, of

* Corresponding author: tannn@huce.edu.vn

http://dx.doi.org/10.28991/CEJ-2022-08-05-07

which 62 million tons were for domestic consumption, while the rest was exported. However, cement production requires a large volume of natural resources and discharges a high volume of $CO_2$ into the atmosphere, leading to environmental pollution and climate change [1–3]. Meanwhile, ground granulated blast furnace slag (GGBFS), a by-product of the process of creating steel, has been widely utilized in the world as a supplementary material to produce concrete [4-6]. It was also applied as a binder material in the production of mortar [7-9]. Furthermore, GGBFS was also used in the mix proportion of other construction materials such as paste [10], self-compacting concrete [11], and foamed concrete [12]. However, the use of GGBFS in the production of construction materials in Vietnam is still limited [13].

As long as urbanization remains a priority, the demand for mortar will keep increasing, especially for important construction projects such as high-rise buildings and coastal structures. The mortars used in these structures are required to have high strength and excellent resistance to chemical attacks. Meanwhile, the most popular high-strength mortars utilized in hydraulic projects in Vietnam have a compressive strength of about 30–50 MPa. Therefore, developing a mortar with a compressive strength of above 50 MPa and excellent durability is necessary. On the other hand, reactive powder concrete (RPC) is well-known as a unique construction material with superior performance compared to ordinary concrete [14–16]. The compositions of RPC contain fine materials such as cement, silica fume, and sand, like mortar compositions. However, the workability of RPC is often really poor due to the low water-to-binder ratio [17]. Recently, high workability and high-strength mortars have been developed based on RPC by increasing the water-to-binder ratio [17, 18] and used as a repair material. With high mechanical strength, these mortars show the potential to be used for important construction or structures working in aggressive environments. However, the studies on this kind of mortar are still limited, and previous studies [17, 18] focused only on the strength of this material. Thus, its durability needs further investigation, especially the resistance to chemical attacks.

In order to encourage the recycling of GGBFS in Vietnam, this study aims to investigate the use of GGBFS to partially replace cement in the production of high-strength mortars containing fine materials like RPC compositions. The effect of GGBFS content on the mechanical and durability properties of high-strength mortars is comprehensively investigated. In addition, the microstructure of this material is also investigated using the scanning electron microscopy (SEM) technique. The obtained results contribute to designing a sustainable material that saves natural resources and recycles a part of the solid waste of iron and steel factories. The detailed experimental procedures are described in Figure 1, and they are presented in the following sections.

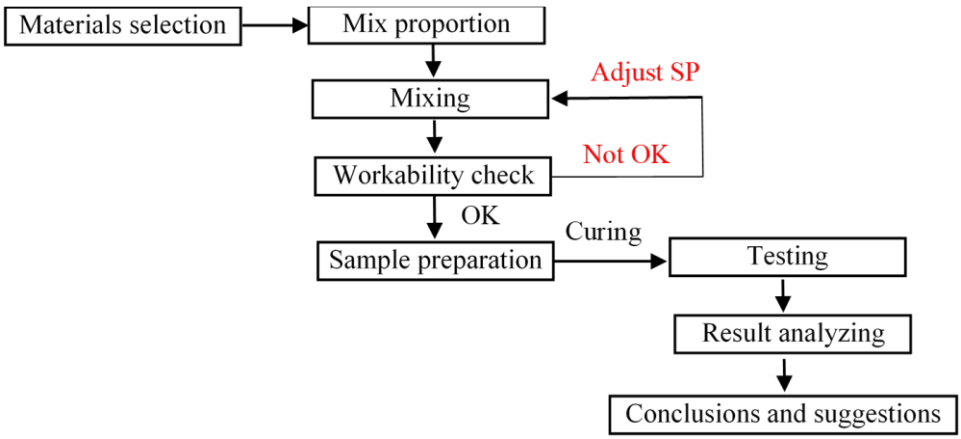


**Figure 1. Experimental procedures**

## 2. Materials and Methods

### 2.1. Materials

Table 1 presents the compositions of all binder materials used to produce high-strength mortars in this study, including cement, silica fume, and GGBFS. In which the cement used is type PCB40, while GGBFS typed S95 is sourced from Hoa Phat's steel factory in Hai Duong province, Vietnam. According to Table 1, the main component of silica fume is silicon dioxide, while the main components of cement and GGBFS are silicon dioxide and calcium oxide. The specific gravities of cement, silica fume, and GGBFS are 3.12, 2.21, and 2.82, respectively. It means that cement has the highest density, followed by GGBFS and then silica fume. The appearances of cement, silica fume, and GGBFS are observed under scanning electron microscopy with a magnification of 1,000 times, as shown in Figures 2-a, 2-b, and 2-c, respectively. The particle shape of cement and GGBFS is irregular, while that of many silica fume particles is spherical. The particle size distributions of these binder materials are shown in Figure 3. It is observed that most GGBFS particles have a diameter of less than 10 $\mu m$, and the particle size of GGBFS is smaller than those of cement and silica fume.

The natural river sand with a density of 2630 kg/m$^3$, a water absorption of 0.42%, and sizes ranging from 0.15 mm to 0.63 mm was used as fine aggregate. It is noticed that the size of sand in the present study is similar to the previous study [19]. The tap water was utilized for mixing. The superplasticizer (SP) type G with a specific gravity of 1.15 was used to control the mortar workability with a flow diameter of around 180±20 mm. This is the typical flow diameter of mortar stipulated by Vietnamese standards.

**Table 1. Chemical compositions of cement, silica fume, and GGBFS**

| Composition (%) | Cement | Silica fume | GGBFS |
|---|---|---|---|
| $SiO_2$ | 22.3 | 90.1 | 36.9 |
| $Al_2O_3$ | 6.7 | 0.98 | 12.4 |
| $Fe_2O_3$ | 4.7 | 1.02 | - |
| CaO | 55.5 | 0.44 | 30.7 |
| MgO | 2.4 | 1.86 | 14.8 |
| $SO_3$ | 1.3 | 0.30 | 0.4 |
| $P_2O_5$ | 0.3 | 0.14 | - |
| Loss on ignition (%) | 0.5 | 1.12 | 0.4 |

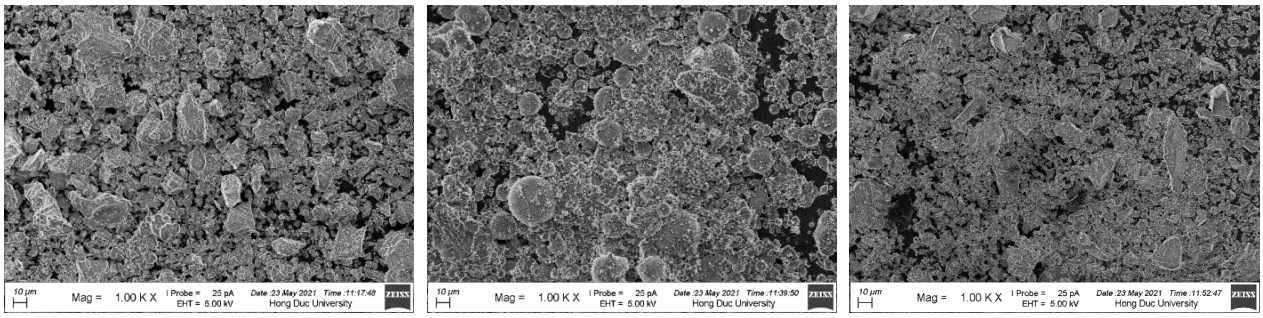

(a) Cement (b) Silica fume (c) GGBFS

**Figure 2. SEM observations of (a) cement, (b) silica fume, and (c) GGBFS**

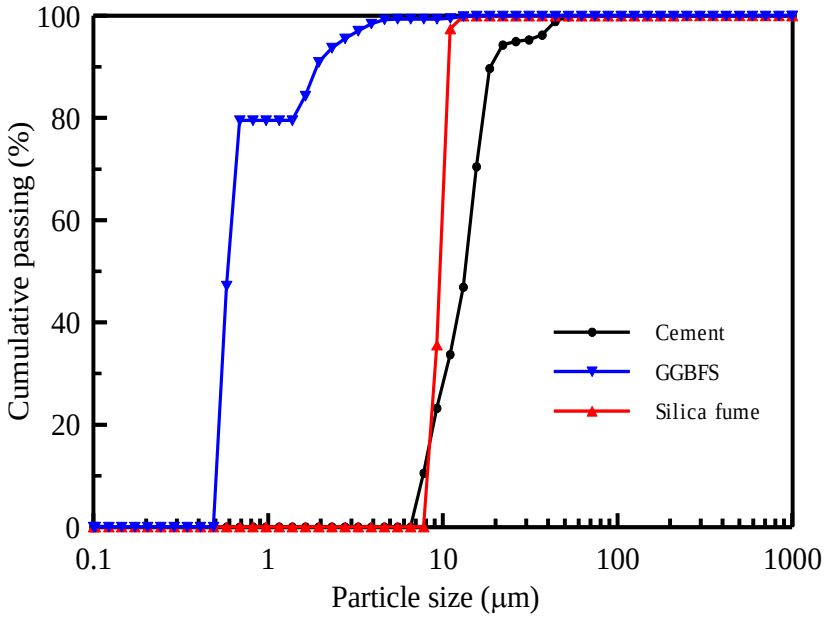


**Figure 3. Particle size distribution of binder materials**

## 2.2. Mixture Proportions

The proportions of all mortar mixtures are presented in Table 2. First, the control mixture without GGBFS, referred to as GG00, was designed with a water-to-binder ratio (W/B) of 0.2, and the amount of silica fume was selected to equal 25% amount of binder by mass. Notably, to get super strength, a low W/B and silica fume content of around 15-25% of the total binder were used in the mixtures [19, 20]. Then, four other mixtures were designed by replacing 15, 30, 45, and

60% of cement content in the control mixture by GGBFS named GG15, GG30, GG45, and GG60, respectively. In addition, the dosage of SP was used to adjust the workability of mortar with flow diameter felt in the range of 180±20 mm. It is noticed that the flow diameter of fresh mortar was measured immediately after mixing, and the SP dosage was also adjusted during the mixing process. The water content given in Table 2 is the calculated value. In practice, the mixing water content has to take into consideration the water absorption and moisture of the sand.

**Table 2. Mix proportions**

| Proportion (kg/m$^3$) | GG00 | GG15 | GG30 | GG45 | GG60 |
|---|---|---|---|---|---|
| Cement | 843.1 | 704.5 | 570.5 | 440.9 | 315.5 |
| Silica fume | 210.8 | 207.2 | 203.8 | 200.4 | 197.2 |
| GGBFS | 0 | 124.3 | 244.5 | 360.8 | 473.3 |
| Sand | 1053.9 | 1036.0 | 1018.8 | 1002.1 | 986.0 |
| Water | 210.8 | 207.2 | 203.8 | 200.4 | 197.2 |
| SP | 26.3 | 25.9 | 25.5 | 25.1 | 24.6 |

## 2.3. Sample Preparation

The mixing process consists of two steps. First, all dry materials, including cement, silica fume, GGBFS, and sand, were mixed together for three minutes [19, 20]. Then, a mixture of water and SP was added and continuously mixed for another six minutes until homogeneity was obtained. After that, the workability of the mortars was checked through the value of flow diameter in accordance with ASTM C1437 [21]. The flow diameter of mortars was controlled in the range of 180±20 mm and adjusted by changing the SP dosage. When the workability of the mixture was satisfied, the mortar mixture was poured into steel molds with different dimensions where it would be prepared as samples using table vibration and hand tamping. All samples were first cured for 24 hours in laboratory conditions. After that, they were de-molded and cured in water at room temperature until the testing days, except for samples used for the drying shrinkage test.

## 2.4. Test Methods

Right after mixing, properties of fresh mortar such as workability and unit weight were measured according to ASTM C1437 [21] and ASTM C138/C138M [22], respectively. The flexural strength test was conducted on prismatic samples with dimensions of 40×40×160 mm in compliance with ASTM C348 [23]. After the fracture, two halves of each sample were used to measure the compressive strength in accordance with ASTM C349 [24]. Flexural and compressive strength tests were conducted simultaneously at 3, 7, 14, 28, and 56 days. While flexural strength was an average value of three sample tests, compressive strength was an average value of six half sample tests.

The cylinder samples with a diameter of 100 mm and a height of 200 mm were prepared for UPV measurements. UPV test is a non-destructive method to evaluate the relative quality of mortar [25, 26]. A portable device, namely MATEST-C369N, with two transducers having a 20-mm diameter and a 200 kHz frequency, was used to measure UPV through the mortar samples, based on ASTM C597 [27], as shown in Figure 4. This test was conducted at 28 and 56 days, and the reported value herein was an average value of at least three samples.

**Figure 4. Ultrasonic pulse velocity test**

Water absorption is related to permeability and resistance of mortar to chemical attack [28]. In this study, cubic samples with dimensions of 50×50×50 mm were used to measure the water absorption capacity of these high-strength mortars complying with ASTM C642 [29]. This test was conducted at 28 and 56 days.

The high content of cement and silica fume is the culprit of micro-cracks that affect the durability properties of mortar [30]. Thus, the drying shrinkage of mortar was tested on prismatic samples with dimensions of 25×25×285 mm based on ASTM C490/C490M [31]. All the samples were placed in the storage cabinet with a temperature of 23±2ºC and a humidity of 50±4%. Test results were recorded for up to 56 days. The zero measurements were set when the samples were de-molded (24 hours after casting). Figure 5 illustrates the samples and the apparatus used for the drying shrinkage measurements.

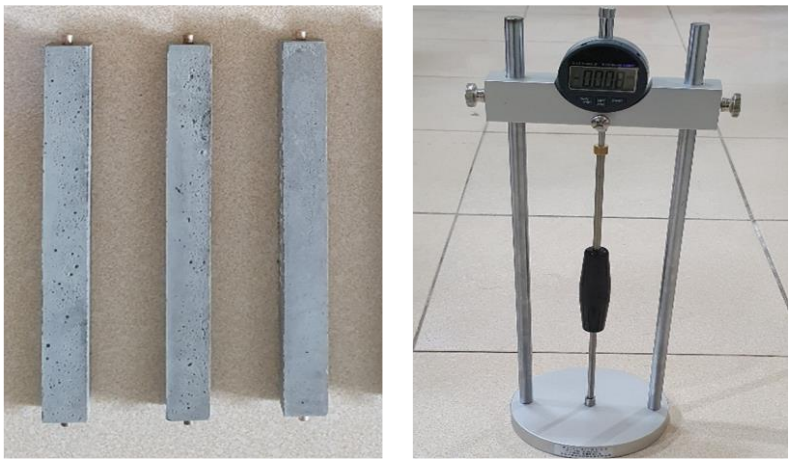

(a) (b)

**Figure 5. (a) Samples and (b) apparatus used for drying shrinkage test**

The chloride attack resistance of mortars was measured by the total charge passed through a cylindrical sample with a 100-mm diameter and a 50-mm height for six hours. The samples in this test were cut from cylinder samples with a 100-mm diameter and a 200-mm height. This test was conducted at 28 and 56 days according to ASTM C1202 [32], as shown in Figure 6.

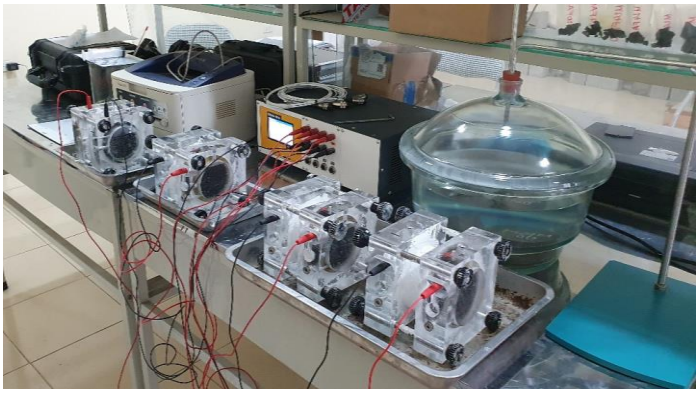

**Figure 6. Rapid chloride ion penetration test**

Fractures of the samples after the compression test at 28 days were used for the microstructure investigation under scanning electron microscopy. The equipment named EVO18 provided by the ZEISS producer, as shown in Figure 7, was used to examine the microstructure of these mortars in this study.


**Figure 7. Scanning electron microscopy test**

# 3. Test Results and Discussions

## 3.1. Properties of Fresh Mortars

Table 3 shows the properties of the fresh mortars, including flow diameter and unit weight. The GGBFS contents are also presented for discussion. It is noticed that the SP dosage is equal to 2.5% for all mortar mixtures, which is calculated as a percentage of the total binder by weight. The flow diameter of mortars increases slightly from 170 mm to 200 mm when the GGBFS content changes from 0% to 60%. This means that the workability of mortar slightly improves as the GGBFS replacement level increases. This finding agrees with a result conducted by Oner and Akyuz [33]. As shown in Figure 3, the particle diameter of GGBFS is smaller than those of cement and silica fume, which acts as a lubricant material, increasing the flowability of the mortar [34]. According to Table 3, the unit weight of mortars reduces slightly as the GGBFS content increases. As aforementioned, the specific gravity of GGBFS is lower than that of cement. Thus, replacing a part of cement with GGBFS reduces the unit weight of the fresh mortar. However, the difference in unit weights of these fresh mortars is marginal and can be ignored.

**Table 3. Properties of fresh mortars**

| Mix | GGBFS content (%) | Flow diameter (mm) | Unit weight (kg/m$^3$) |
|---|---|---|---|
| GG00 | 0 | 170 | 2244 |
| GG15 | 15 | 175 | 2239 |
| GG30 | 30 | 181 | 2227 |
| GG45 | 45 | 192 | 2202 |
| GG60 | 60 | 200 | 2163 |

## 3.2. Compressive Strength

The compressive strength development of the mortars with different GGBFS contents is shown in Figure 8. The compressive strength of the control mix mixture at 56 days is 109.7 MPa. The 56-day compressive strengths of the mixtures using 15, 30, 45, and 60% GGBFS substitutions are 127.5, 115.7, 105.4, and 98.1 MPa, respectively. It means that replacing 15 or 30% of cement with GGBFS increases the compressive strength of mortar. A previous study [35] has indicated that the filler effect (due to the very small size) and the pozzolanic effect of GGBFS contribute to increased compressive strength in mortar. Therefore, if the amount of GGBFS used is optimal, GGBFS can fill in the voids and make the mortar microstructure denser, increasing the compressive strength. On the other hand, when the GGBFS content increases over the optimal value, the compressive strength of mortar reduces. However, all mortars in this study have a compressive strength of above 98 MPa at 56 days, which is significantly higher than conventional cement mortars used in practice with a common compressive strength of around 20-50 MPa.

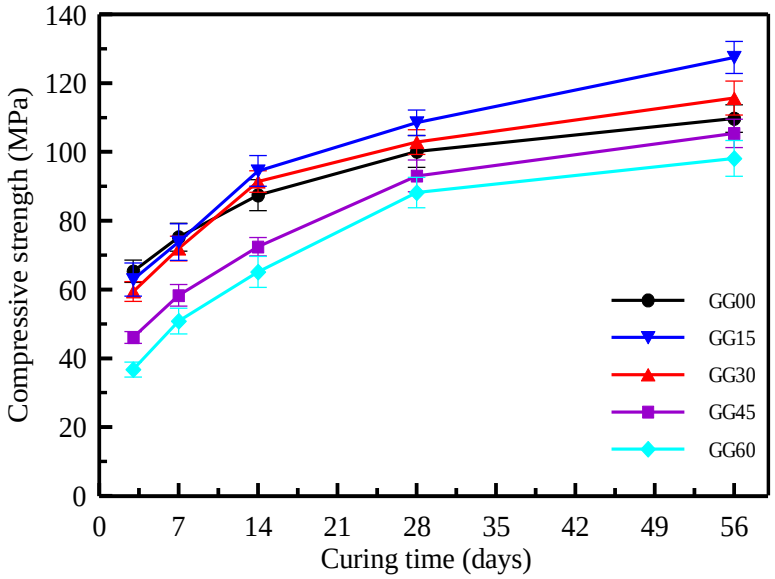


**Figure 8. Compressive strength of the mortars with various GGBFS contents**

The compressive strengths of the mortars used in this study are higher than those values reported by Yun et al. [7] and Liu and Huang [17]. It is noticed that Yun et al. [7] used GGBFS to replace 20, 40, and 50% of cement in producing conventional mortars, while Liu and Huang [17] increased the water-to-binder ratio to 0.28 in the production of the high flowable mortar. The higher compressive strength of mortar in this study compared to the values reported by Yun et al.

[7] is due to the presence of silica fume. Meanwhile, the lower water-to-binder ratio results in a mortar compressive strength higher than that reported in Liu and Huang's study [17]. However, the compressive strength of the mortars in this study is lower than the compressive strength of RPC conducted by Yazici et al. [36]. Furthermore, it is noticed that the samples tested were cured in water at room temperature as standard condition, while the samples in Yazici's study [36] were cured in autoclave condition with high temperature and pre-pressure. Under high temperatures, all binder materials are more activated than under standard conditions. This will be discussed in the next section by using SEM observation.

### 3.3. Flexural Strength

Figure 9 shows the flexural strength development of the mortars with various GGBFS contents. Similar to compressive strength, the flexural strength of the mixtures using 15 and 30% GGBFS is higher than that of the control mixture, while the flexural strength of the mixtures using 45 and 60% GGBFS is lower than that of the control mixture. Thus, the use of 15 or 30% GGBFS is considered an optimal cement replacement level. Yazici et al. [36] have concluded that replacing 20% or 40% cement with GGBFS yields an increase in the flexural strength of RPC. This phenomenon may be due to the improved bond between GGBFS and other materials, thus improving the bond strength between mortar matrices [36].

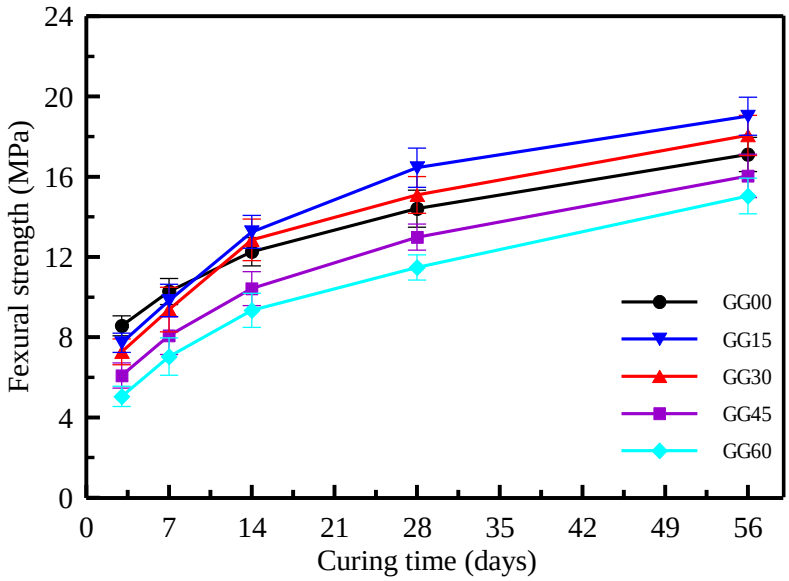


**Figure 9. Flexural strength of the mortars with various GGBFS contents**

On the other hand, the filler effect and the pozzolanic effect of GGBFS [35] are also responsible for the improved flexural strength of mortars using the mineral admixtures. At 28 days, the flexural strength of these mortars ranges from 11.5 to 16.5 MPa. At 56 days, these flexural strengths boost to 15-19 MPa, similar to the values reported by Yazici et al. [37]. It is noticed that both samples in the present study and Yazici's study [37] were cured in standard water conditions. On the other hand, the cement-based mortar containing GGBFS conducted by Yun et al. [7] had a flexural strength of lower than 12 MPa, which is lower than the flexural strength of those mortars produced in this study. The higher flexural strength is a result of adding silica fume into the mix proportion. However, the flexural strength of these mortars is lower than that of RPC conducted by Yiğiter et al. [38], which is cured under autoclave conditions. Yazici et al. [37] stated that concrete cured in a pre-pressure and high temperature had higher strength than concrete cured under the standard condition.

### 3.4. Ultrasonic Pulse Velocity (UPV)

Figure 10 shows the UPV values through the mortar samples with various GGBFS contents at 28 and 56 days. It shows that the UPV value increases as the age of mortars increases and reduces as the GGBFS content increases. A previous study conducted by Bogas et al. [39] has indicated that the density of the sample has a strong effect on the UPV values. The sample with high density often results in a high UPV value. In this study, when replacing cement with GGBFS, the unit weight of mortar was slightly reduced and thus resulting in the UPV value of these samples being lower than that of the control sample. However, the difference in UPV between the GG15 and GG30 mixtures and the control mixture (GG00) is slight. That is because the unit weights of the GG15 and GG30 mixtures are slightly smaller than that of the GG00 mixture. The considerable variation is for mixtures with high GGBFS content (GG45 and GG60). All mortar samples at 28 days exhibit UPV values higher than 4200 m/s. Solís-Carcaño and Moreno [40] stated that the quality of concrete is good if its UPV value is higher than 4100 m/s. Therefore, all mortars tested in this study show good quality.

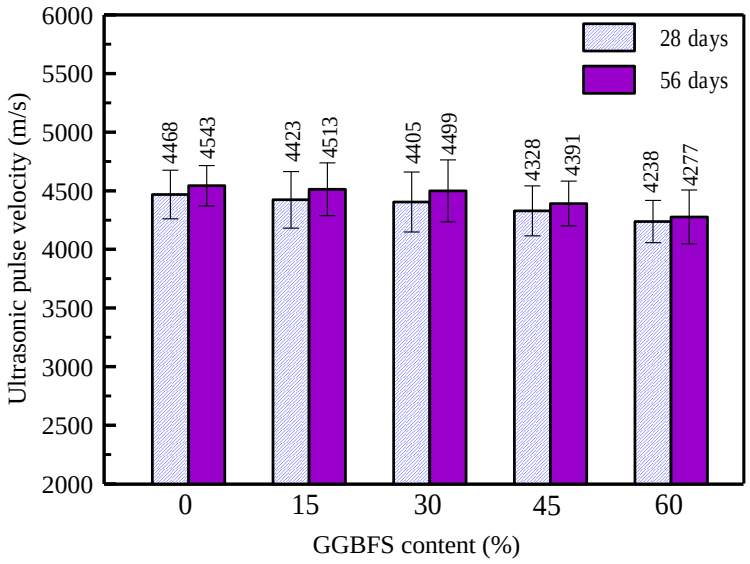


**Figure 10. UPV in the mortars with various GGBFS contents**

## 3.5. Water Absorption

The water absorptions of all mortars at 28 and 56 days are shown in Figure 11. The water absorption at 56 days is significantly reduced compared to that at 28 days. This phenomenon is associated with the increase in hydration products over time, resulting in a denser microstructure followed by reduced water absorption. The mixtures with 15 and 30% GGBFS content show lower water absorption than the control mixture. However, when the GGBFS content increases from 45 to 60%, the water absorption of these samples is at a higher value than that of the control mixture. It means that the use of 15 to 30% GBBFS as cement replacement is optimal, as aforementioned. As stated in the previous study [35, 36], the benefits of using GGBFS are the filler and pozzolanic effects, which minimize the capillary pores, thus reducing the water absorption. At 56 days, the water absorption of these mortars ranges from 1.16% to 2.16%, which is significantly lower than the reported values from a previous study [41], indicating good quality. The water absorption capacity is often related to the permeable capacity and chemical attack resistance of mortar [28]. If the water absorption is low, the permeability of mortar is also low, and thus the resistance to chemical ingression is high.

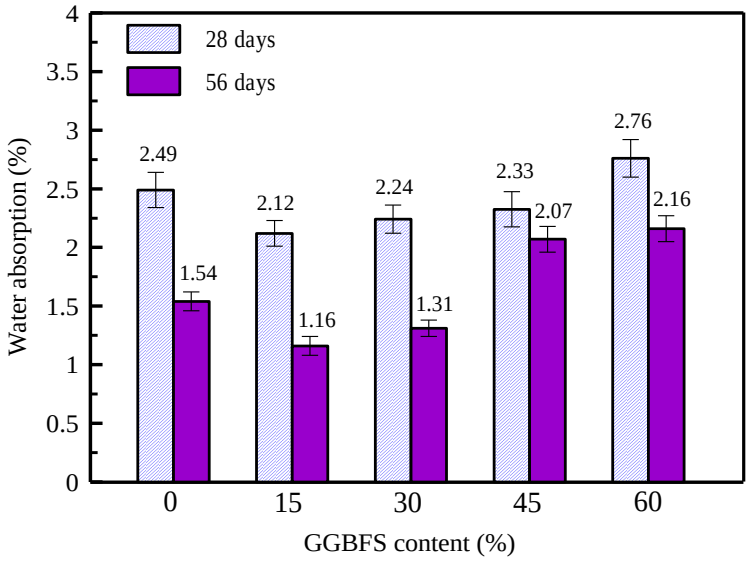


**Figure 11. Water absorption of the mortars with various GGBFS contents**

## 3.6. Drying Shrinkage

The drying shrinkage is one of the major problems if the low W/B ratio and high content of cement and silica fume are used [30]. Since the drying shrinkage is high, the appeared micro-cracks negatively influence the durability of mortar, especially its resistance to corrosive chemical agents that easily penetrate the mortar through these micro-cracks. In this study, the drying shrinkage was evaluated through the length change of the prismatic samples with dimensions of 25×25×285 mm, as shown in Figure 12. It shows that the drying shrinkage increases rapidly from the beginning to 14 days of age and then gradually slows down. This result is due to the hydration that has a high reaction rate in the first stage and lower rates in the later stages.

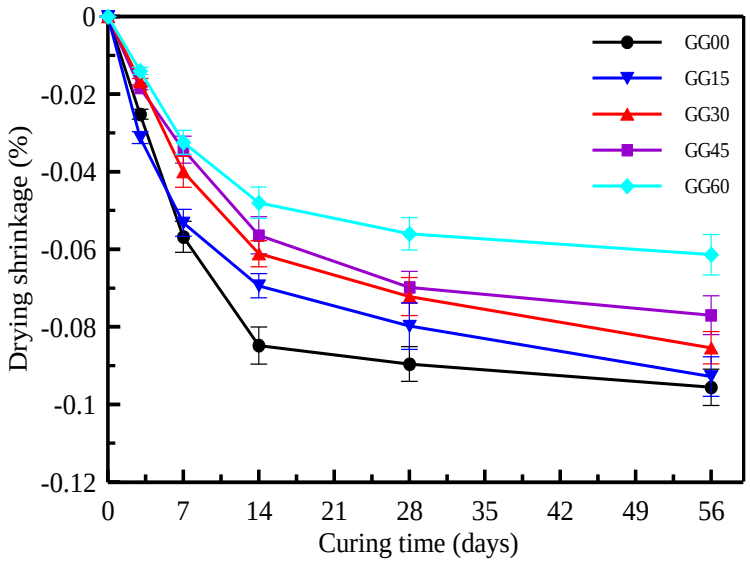


**Figure 12. Length change of the mortars with various GGBFS contents**

In addition, the drying shrinkage of the mortars reduces when the BBGFS content increases. It is noticed that the filler effect of GGBFS [36] results in the reduction of porosity inside the mortar and the drying shrinkage. On the other hand, the pozzolanic reaction of GGBFS releases lower heat than the hydration reaction of cement. This also helps to reduce the drying shrinkage of mortar. Furthermore, Kou et al. [35] have concluded that using mineral admixtures such as fly ash and GGBFS resulted in reducing drying shrinkage. In other words, the use of GGBFS can reduce the drying shrinkage of mortars.

### 3.7. Rapid Chloride Ion Penetration (RCPT)

The ability of the mortar to resist the penetration of chloride ions is assessed through the total charge passed through the cylinder samples with a diameter of 100 mm and a height of 50 mm during six hours. Test results on the mortar samples at 28 and 56 days are presented in Figure 13.

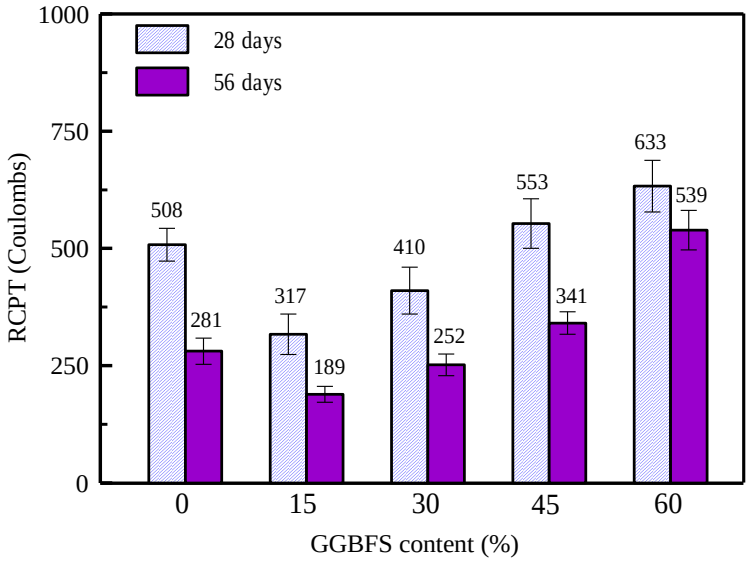


**Figure 13. Total charge passed through the mortars with various GGBFS content**

At 28 days, the total charge passed through the mortar samples ranges from 317 to 633 Coulombs corresponding to the GGBFS increase from 0% to 60%. However, these values were significantly reduced at 56 days. Moreover, the sample with 15% GGBFS was the most effective at preventing the ingression of chloride ions, followed by the samples with 30% GGBFS. The mixture using GGBFS to replace 60% of cement content (GG60) shows a higher RCPT value than the control mixture (GG00). The improvement of resistance to chloride ion attack over time is due to the formation of hydration products during curing time. This is explained by the lower values of RCPT measured at 56 days compared to those at 28 days. Several studies [35, 42, 43] have indicated that the use of mineral admixture is effective in resisting chloride ion penetration. The improvement in impermeability by using GGBFS leads to the enhancement in resistance

to chloride attack. Luo et al. [42] have found that using GGBFS can significantly improve the durability of concrete, especially in reducing chloride diffusion, thanks to the reduced capillary pores. In the present study, the samples with 15% and 30% GGBFS exhibited lower water absorption (as shown in Figure 11), and thus these samples also showed high resistance to penetration of chloride ions [28]. Furthermore, all mortars in this study have a 56-day RCPT value of below 1,000 Coulombs, indicating the high resistance to chloride attack as stipulated by ASTM C1202 [32]. Based on the test results of UPV, water absorption, drying shrinkage, and RCPT, these mortars in this study have good durability, especially against chloride ion attack.

### 3.8. SEM Observation

The SEM images of all mortars are shown in Figure 14. The microstructures of these samples are dense and similar, and there is not much difference between SEM images. However, it is interesting that several free silica fumes with a spherical shape were observed, indicating that not all silica fume particles participated in the hydration reaction. This finding explains the lower compressive strength and flexural strength of the mortars in this study compared to those values reported in previous studies [36, 38]. It is noticed that the samples in Yazici's study [36] and Yiğiter's study [38] were cured in autoclave conditions with high temperature and pre-pressure. Thus, most binder particles were activated and joined in the hydration or pozzolanic reaction, resulting in high compressive and flexural strengths. Yazici et al. [36] have also mentioned that the curing condition has a strong effect on the properties of concrete. The strength of the sample curing in autoclave conditions was significantly higher than that of the sample curing in standard conditions. However, the autoclave curing condition requires more modern equipment, which increases the construction cost. Therefore, it is not effective to apply in practice. On the other hand, all mortar samples in this study were cured in water under indoor environmental conditions. Although the mechanical strengths of these samples were not as high as the samples cured in autoclave conditions, all mortars tested still show a high compressive strength (above 98 MPa) and a high flexural strength (above 15 MPa).

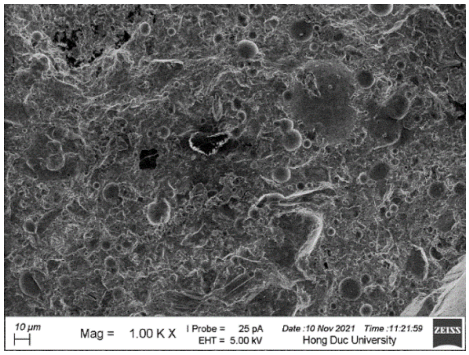


(a) GG00

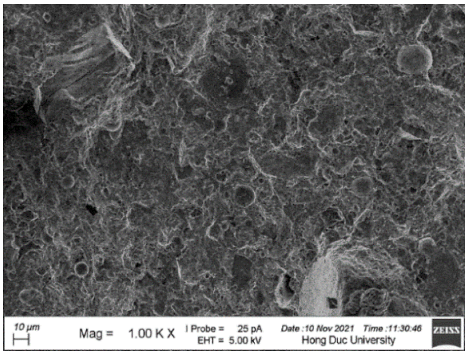


(b) GG15

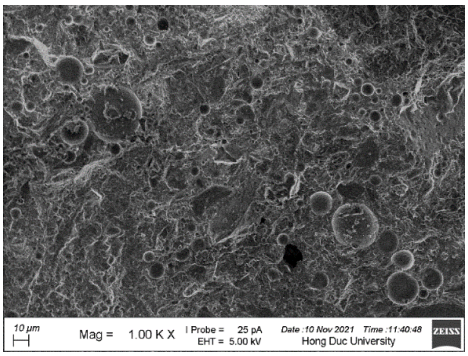


(c) GG30

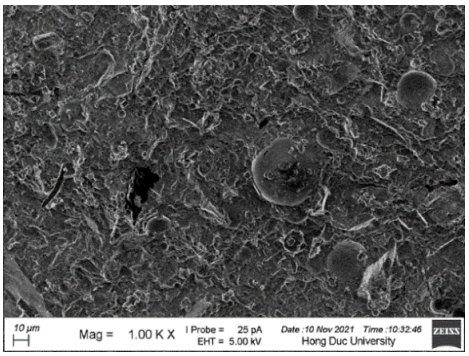


(d) GG45

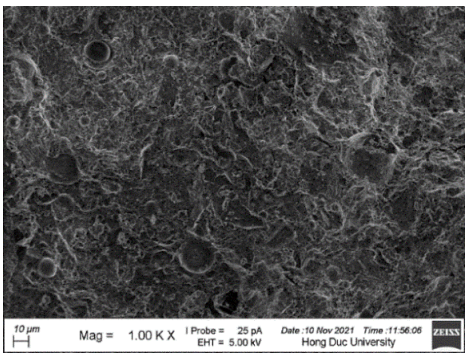


(e) GG60

**Figure 14. SEM observations of the mortars**

## 4. Conclusions

In this study, the high-strength mortars have been designed and tested for assessing the effect of several GGBFS contents. The GGBFS was used to replace 0, 15, 30, 45, and 60% of the cement content by mass. A series of tests were carried out on the mortar samples in the laboratory. The main conclusions that can be drawn from the obtained results are as follows:

- The use of GGBFS to replace 15 or 30% of the cement content resulted in increasing the compressive strength and flexural strength, reducing the water absorption and RCPT values compared to the control mixture with free-GGBFS.
- The unit weight, drying shrinkage, and UPV values of the mortars were reduced as the GGBFS content increased.
- All the mortars tested exhibited good quality with high compressive (above 98 MPa) and flexural strength (above 15 MPa), high UPV (above 4200 m/s), low water absorption (below 2.76%), low drying shrinkage (below 0.1%), and high resistance to chloride attack (RCPT value of less than 1,000 Coulombs).
- The microstructure observation of the mortars studied under scanning electron microscopy was dense. However, some free silica fume particles were detected, indicating that not all silica fume jointed the hydration reaction under standard curing conditions.
- The use of GGBFS in the production of the reactive powder mortars offers a way to treat a part of solid waste from iron and steel factories, which also helps save natural resources.
- With high mechanical strength and high resistance to chemical attack, the mortars produced in this study can be used as high-strength mortars or as materials used for the rehabilitation of hydraulic structures.

## 5. Declarations

### 5.1. Author Contributions

Conceptualization: S.H.N. and N.T.N.; methodology: S.H.N.; validation: S.H.N., N.T.N. and X.H.N.; formal analysis: S.H.N.; investigation: S.H.N., X.H.N. and N.T.N.; resources: S.H.N.; data curation: N.T.N.; writing—original draft preparation: N.T.N. and X.H.N.; writing—review and editing: S.H.N. and N.T.N.; visualization: S.H.N.; supervision: N.T.N.; project administration: X.N.H.; funding acquisition: N.T.N. and X.H.N. All authors have read and agreed to the published version of the manuscript.

### 5.2. Data Availability Statement

The data presented in this study are available in the article.

### 5.3. Funding

The authors received no financial support for the research, authorship, and/or publication of this article.

### 5.4. Acknowledgements

The present study is supported by the Ministry of Construction, Vietnam, under grant number RD 57-19. The authors would like to thank Ms. Le Thi Thanh Tam and Ms. Mai Thi Ngoc Hang for their support during the experiment.

### 5.5. Conflicts of Interest

The authors declare no conflict of interest.

## 6. References

[1] Malhotra, V. M. (2002). Introduction: Sustainable Development and Concrete Technology. Concrete International, 24(7), 1-22.

[2] Cheah, C. B., Part, W. K., & Ramli, M. (2015). The hybridizations of coal fly ash and wood ash for the fabrication of low alkalinity geopolymer load bearing block cured at ambient temperature. Construction and Building Materials, 88, 41–55. doi:10.1016/j.conbuildmat.2015.04.020.

[3] Chindaprasirt, P., Jaturapitakkul, C., Chalee, W., & Rattanasak, U. (2009). Comparative study on the characteristics of fly ash and bottom ash geopolymers. Waste Management, 29(2), 539–543. doi:10.1016/j.wasman.2008.06.023.

[4] Kumar, G., & Mishra, S. S. (2021). Effect of ggbfs on workability and strength of alkali-activated geopolymer concrete. Civil Engineering Journal (Iran), 7(6), 1036–1049. doi:10.28991/cej-2021-03091708.

[5] Shehata, N., Mohamed, O. A., Sayed, E. T., Abdelkareem, M. A., & Olabi, A. G. (2022). Geopolymer concrete as green building materials: Recent applications, sustainable development and circular economy potentials. Science of the Total Environment, 836, 155577. doi:10.1016/j.scitotenv.2022.155577.

[6] Borrero, E. L. S., Farhangi, V., Jadidi, K., & Karakouzian, M. (2021). An Experimental Study on Concrete's Durability and Mechanical Characteristics Subjected to Different Curing Regimes. Civil Engineering Journal, 7(4), 676–689. doi:10.28991/cej-2021-03091681.

[7] Yun, C. M., Rahman, M. R., Phing, C. Y. W., Chie, A. W. M., & Bakri, M. K. Bin. (2020). The curing times effect on the strength of ground granulated blast furnace slag (GGBFS) mortar. Construction and Building Materials, 260, 120662. doi:10.1016/j.conbuildmat.2020.120622.

[8] Aydin, S. (2013). A ternary optimisation of mineral additives of alkali activated cement mortars. Construction and Building Materials, 43, 131–138. doi:10.1016/j.conbuildmat.2013.02.005.

[9] Delhomme, F., Ambroise, J., & Limam, A. (2012). Effects of high temperatures on mortar specimens containing Portland cement and GGBFS. Materials and structures, 45(11), 1685-1692. doi:10.1617/s11527-012-9865-7.

[10] Vanoutrive, H., Minne, P., Van de Voorde, I., Cizer, Ö., & Gruyaert, E. (2022). Carbonation of cement paste with GGBFS: Effect of curing duration, replacement level and CO2 concentration on the reaction products and CO2 buffer capacity. Cement and Concrete Composites, 129, 104449. doi:10.1016/j.cemconcomp.2022.104449.

[11] Sahoo, K. K., Dhir, P. K., Behera, S. K., & Biswal, D. R. (2022). Influence of Ground-Granulated Blast-Furnace Slag on the Structural Performance of Self-Compacting Concrete. Practice Periodical on Structural Design and Construction, 27(3), 4022019. doi:10.1061/(asce)sc.1943-5576.0000697.

[12] Jose, S. K., Soman, M., & Sheela Evangeline, Y. (2021). Ecofriendly building blocks using foamed concrete with ground granulated blast furnace slag. International Journal of Sustainable Engineering, 14(4), 776–784. doi:10.1080/19397038.2020.1836064.

[13] Ngo, S. H., & Huynh, T. P. (2022). Effect of paste content on long-term strength and durability performance of green mortars. Journal of Science and Technology in Civil Engineering (STCE)-HUCE, 16(1), 113–125. doi:10.31814/stce.huce(nuce)2022-16(1)-10.

[14] Zheng, W., Luo, B., & Wang, Y. (2013). Compressive and tensile properties of reactive powder concrete with steel fibres at elevated temperatures. Construction and Building Materials, 41, 844–851. doi:10.1016/j.conbuildmat.2012.12.066.

[15] Canbaz, M. (2014). The effect of high temperature on reactive powder concrete. Construction and Building Materials, 70, 508–513. doi:10.1016/j.conbuildmat.2014.07.097.

[16] Hiremath, P. N., & Yaragal, S. C. (2018). Performance evaluation of reactive powder concrete with polypropylene fibers at elevated temperatures. Construction and Building Materials, 169, 499–512. doi:10.1016/j.conbuildmat.2018.03.020.

[17] Liu, C. T., & Huang, J. S. (2009). Fire performance of highly flowable reactive powder concrete. Construction and Building Materials, 23(5), 2072–2079. doi:10.1016/j.conbuildmat.2008.08.022.

[18] Lee, M. G., Wang, Y. C., & Chiu, C. T. (2007). A preliminary study of reactive powder concrete as a new repair material. Construction and Building Materials, 21(1), 182–189. doi:10.1016/j.conbuildmat.2005.06.024.

[19] Peng, Y., Zhang, J., Liu, J., Ke, J., & Wang, F. (2015). Properties and microstructure of reactive powder concrete having a high content of phosphorous slag powder and silica fume. Construction and Building Materials, 101, 482–487. doi:10.1016/j.conbuildmat.2015.10.046.

[20] Cwirzen, A., Penttala, V., & Vornanen, C. (2008). Reactive powder based concretes: Mechanical properties, durability and hybrid use with OPC. Cement and Concrete Research, 38(10), 1217–1226. doi:10.1016/j.cemconres.2008.03.013.

[21] ASTM C1437-15. (2020). Standard Test Method for Flow of Hydraulic Cement Mortar. ASTM International, Pennsylvania, United States. doi:10.1520/C1437-15.

[22] ASTM C138/C138M-17a. (2017). Standard Test Method for Density (Unit Weight), Yield, and Air Content (Gravimetric). ASTM International, Pennsylvania, United States. doi:10.1520/C0138_C0138M-17A.

[23] ASTM C348-21. (2021). Standard Test Method for Flexural Strength of Hydraulic-Cement Mortars. ASTM International, Pennsylvania, United States. doi:10.1520/C0348-21.

[24] ASTM C349-18. (2018). Standard Test Method for Compressive Strength of Hydraulic-Cement Mortars (Using Portions of Prisms Broken in Flexure). ASTM International, Pennsylvania, United States. doi:10.1520/C0349-18.

[25] Nguyen, N. T., Sbartaï, Z. M., Lataste, J. F., Breysse, D., & Bos, F. (2013). Assessing the spatial variability of concrete structures using NDT techniques - Laboratory tests and case study. Construction and Building Materials, 49, 240–250. doi:10.1016/j.conbuildmat.2013.08.011.

[26] Nguyen, N. T., Sbartaï, Z. M., Lataste, J. F., Breysse, D., & Bos, F. (2015). Non-destructive evaluation of the spatial variability of reinforced concrete structures. Mechanics and Industry, 16(1), 103. doi:10.1051/meca/2014064.

[27] ASTM C597-16. (2016). Standard Test Method for Pulse Velocity through Concrete. ASTM International, Pennsylvania, United States. doi:10.1520/C0597-16.

[28] Zhang, S. P., & Zong, L. (2014). Evaluation of Relationship between Water Absorption and Durability of Concrete Materials. Advances in Materials Science and Engineering, 2014, 1–8. doi:10.1155/2014/650373.

[29] ASTM C642-21. (2022). Standard Test Method for Density, Absorption, and Voids in Hardened Concrete, ASTM International, Pennsylvania, United States. doi:10.1520/C0642-21.

[30] Zhang, M. H., Tam, C. T., & Leow, M. P. (2003). Effect of water-to-cementitious materials ratio and silica fume on the autogenous shrinkage of concrete. Cement and Concrete Research, 33(10), 1687–1694. doi:10.1016/S0008-8846(03)00149-2.

[31] ASTM C 490/C490M-21. (2021). Standard Practice for Use of Apparatus for the Determination of Length Change of Hardened Cement Paste, Mortar, and Concrete. ASTM International, Pennsylvania, United States. doi:10.1520/C0490_C0490M-21.

[32] ASTM C1202-19. (2022). Standard Test Method for Electrical Indication of Concrete's Ability to Resist Chloride Ion Penetration. ASTM International, Pennsylvania, United States. doi:10.1520/C1202-19.

[33] Oner, A., & Akyuz, S. (2007). An experimental study on optimum usage of GGBS for the compressive strength of concrete. Cement and Concrete Composites, 29(6), 505–514. doi:10.1016/j.cemconcomp.2007.01.001.

[34] Siddique, R., & Bennacer, R. (2012). Use of iron and steel industry by-product (GGBS) in cement paste and mortar. Resources, Conservation and Recycling, 69, 29–34. doi:10.1016/j.resconrec.2012.09.002.

[35] Kou, S. C., Poon, C. S., & Agrela, F. (2011). Comparisons of natural and recycled aggregate concretes prepared with the addition of different mineral admixtures. Cement and Concrete Composites, 33(8), 788–795. doi:10.1016/j.cemconcomp.2011.05.009.

[36] Yazici, H., Yardimci, M. Y., Yiğiter, H., Aydin, S., & Türkel, S. (2010). Mechanical properties of reactive powder concrete containing high volumes of ground granulated blast furnace slag. Cement and Concrete Composites, 32(8), 639–648. doi:10.1016/j.cemconcomp.2010.07.005.

[37] Yazici, H., Deniz, E., & Baradan, B. (2013). The effect of autoclave pressure, temperature and duration time on mechanical properties of reactive powder concrete. Construction and Building Materials, 42, 53–63. doi:10.1016/j.conbuildmat.2013.01.003.

[38] Yigiter, H., Aydin, S., Yazici, H., & Yardimci, M. Y. (2012). Mechanical performance of low cement reactive powder concrete (LCRPC). Composites Part B: Engineering, 43(8), 2907–2914. doi:10.1016/j.compositesb.2012.07.042.

[39] Bogas, J. A., Gomes, M. G., & Gomes, A. (2013). Compressive strength evaluation of structural lightweight concrete by non-destructive ultrasonic pulse velocity method. Ultrasonics, 53(5), 962–972. doi:10.1016/j.ultras.2012.12.012.

[40] Solís-Carcaño, R., & Moreno, E. I. (2008). Evaluation of concrete made with crushed limestone aggregate based on ultrasonic pulse velocity. Construction and Building Materials, 22(6), 1225–1231. doi:10.1016/j.conbuildmat.2007.01.014.

[41] Hatungimana, D., Taşköprü, C., İçhedef, M., Saç, M. M., & Yazıcı, Ş. (2019). Compressive strength, water absorption, water sorptivity and surface radon exhalation rate of silica fume and fly ash based mortar. Journal of Building Engineering, 23, 369–376. doi:10.1016/j.jobe.2019.01.011.

[42] Luo, R., Cai, Y., Wang, C., & Huang, X. (2003). Study of chloride binding and diffusion in GGBS concrete. Cement and Concrete Research, 33(1), 1–7. doi:10.1016/S0008-8846(02)00712-3.

[43] Yeau, K. Y., & Kim, E. K. (2005). An experimental study on corrosion resistance of concrete with ground granulate blast-furnace slag. Cement and Concrete Research, 35(7), 1391–1399. doi:10.1016/j.cemconres.2004.11.010.